Development and Control of a Bowden-Cable Actuated Exoskeleton for Upper-Limb Rehabilitation

Qingcong Wu, Xingsong Wang, Fengpo Du, Jigang Xu
School of Mechanical Engineering, Southeast University
Nanjing, China
E-mail: xswang@seu.edu.cn

***Abstract*—This paper deals with the development and control of an upper limb exoskeleton used for the robotic rehabilitation of stroke patients. Bowden-cable actuators with a high power-weight ratio are applied in the robot system to provide remote power transmission and simplify the mechanical design. The kinematics model of the exoskeleton is analyzed and optimized to eliminate singularities from the desired workplace and achieve natural human-robot interaction. A real-time control system is established in xPC target environment and used to process the feedback signals from the force sensor and potentiometers and execute the control algorithm. An impedance control scheme is developed to provide interactive therapy training to the patients with different disability levels. Preliminary experiments have been carried out in two different training modes to evaluate the performance of the proposed exoskeleton and control approach.**

Keywords—upper-limb exoskeleton; rehabilitation; kinematics; real-time control system; impedance control

I. INTRODUCTION

According to the statistical data of the National Stroke Academy, nowadays, there are more than ten million people suffering from the effects of stroke in China and, besides, two million new occurrences every year. Hemiparesis is one of the most serious symptoms of stroke which commonly leads to significant residual physical and cognitive impairment problems. Approximately three quarters of the stroke population survive and require a prolonged physical therapy to regain motor function and improve movement coordination in activities of daily living (ADL) [1]. Researches in clinical treatment show that practicing repetitive multi-joint movement is conductive to the motor recovery. Customarily, physical therapists help the patients to perform different types of functional programs and prevent secondly complications such as muscle atrophy and joint spasticity. However, the therapist treatment is costly and labor-intensive, as it requires one-on-one treatment and, the training durations always take a lot of time. It is a challenge for the therapists to manually remove heavy limbs and quantitatively monitor the therapy progress. To overcome these limitations and maximize the quality of rehabilitation, physical therapy using robotic equipment has garnered significant attention.

In recent years, several kinds of upper-limb robotic rehabilitation systems have been developed to offer body-weight supported training for the stroke patients, and the effectiveness of the robot-assisted therapy on motor recovery has been analyzed and verified [2]. Massachusetts Institute of Technology (MIT) developed a motor driven five-bar-linkage device, named MIT MANUS, to provide five degrees of freedom (DOF) for the elbow, forearm, and wrist motion and achieve predefined force, stiffness, and impedance at the end-effector during target-matching game [3]. The Mirror Image Movement Enabler (MIME) is a robotic device incorporating a PUMA 560 manipulator and can be used for shoulder and elbow rehabilitation. It provides assistance to the impaired limb during unilateral and bilateral movement trainings in three-dimensional space [4]. Zurich University in Switzerland developed a six DOFs upper-limb exoskeleton named ARMin to improve and evaluate the performance of neuromuscular disorder therapy in clinics. The device was equipped with DC motors, encoders and force/torque sensors for the purpose of implementing human-robot interaction training strategies [5]. These active assistive devices are all equipped with driving elements (such as motors and hydraulic cylinders) and, therefore, have some drawbacks in common, such as heavy weight, high inertia, large energy consumption, and potential fail-safe problems. Many other active therapy robots have been designed, such as MGA [6], ARM-100 [7], GENTLE/s [8], L-Exos [9], and IntelliArm [10].

The Wilmington robotic exoskeleton (WREX) is a kind of passive, i.e. non-motorised, rehabilitation system, which makes use of linear elastic elements and auxiliary parallel links to achieve gravity balanced [11]. The WREX cannot supply actuating force to the upper limb. Instead, it keeps the entire upper limb therapy system in balanced state and, as a result, allows the patients to practice appropriate movement patterns with little torque under their own control. However, it is not suitable for the seriously disabled patients due to unavoidable balance errors and friction. ARMON [12] and Dampace [13] are two other types of passive rehabilitation robots.

In this paper, we present the development of a seven DOFs gravity balanced upper limb exoskeleton specialized for the rehabilitation of the shoulder and elbow of stroke patients. DC servo motors and flexible Bowden-cable transmission systems are incorporated into the exoskeleton system in order to simplify the structural design. The joint positions and human-robot interaction forces at the end-effector are measured with potentiometers and force/torque sensor simultaneously for real-time analysis and control. The mechanical design and the

978-1-4799-4926-7/14/$31.00 ©2014 IEEE

configuration space kinematics are described in Section II. For the control of the exoskeleton, a real-time control system is established in xPC target environment based on Matlab/RTW, as shown in Section III. Section IV presents the development of an impedance control scheme and several preliminary experiments and results. Finally, a brief conclusion and future work are made in Section V.

II. Design of The Exoskeleton

A. Mechanical design

To achieve good performance of rehabilitation treatment, the mechanical structure of the exoskeleton is characterized by a serial kinematics to imitate the human arm, as shown in Fig. 1. The exoskeleton has three active DOFs at the shoulder (internal/external, abduction/adduction, and flexion/extension), one active DOF at the elbow (flexion/extension), and one passive DOF at the forearm (pronation/supination). However, it is worth noting that it is unreasonable to simply describe the human shoulder as a ball and socket joint, as the rotation center of glenohumeral joint shifts according to shoulder girdle movement, and the undesired misalignment between robot and human will result in unnatural restraints to the user [14], [15]. Therefore, the exoskeleton is mounted on a two DOFs passive mobile platform to eliminate the misalignment generated in two horizontal directions.

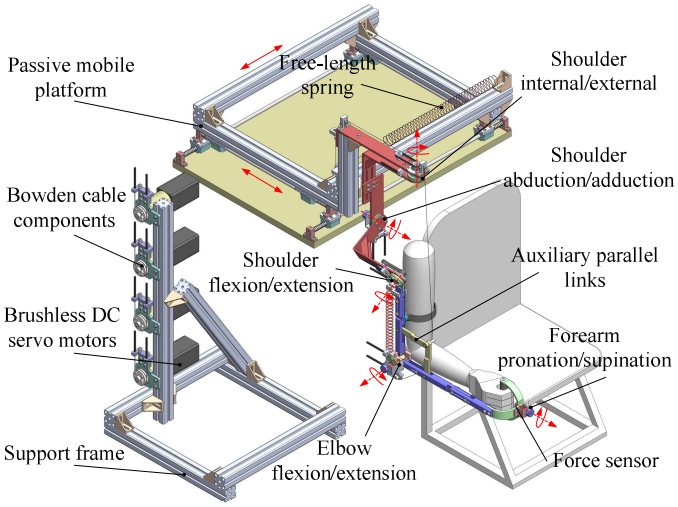

Fig. 1. Major mechanical components of the rehabilitation exoskeleton with human arm.

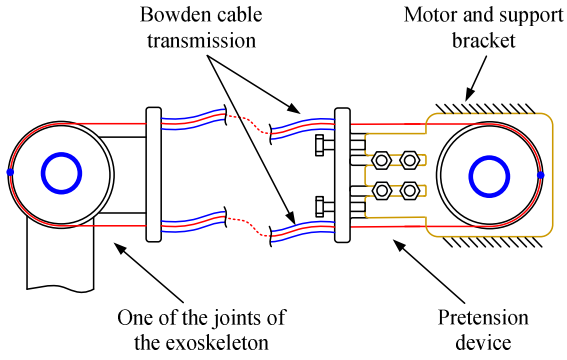

Fig. 2. Bowden-cable transmission system

Each active joint of the exoskeleton is actuated by a servo brushless DC motor (BLDC-56PA77G, reduction ratio-50:1) via a Bowden-cable transmission system, which is constructed as a rotation joint to transfer the driving torque from the actuator to the output side, as shown in Fig. 2. The cables are fastened to the pulleys at the proximal side and distal side in a pull-pull configuration. The system pretension can be adjusted via the pretension device to keep the cables in the pulleys slot. The motors are placed on a support frame remote from the rehabilitation device. The joint positions are detected with angular potentiometers (WDJ22A). A three axes strain gauge-type force/torque sensor (NANO-25-ATI) is attached to the end-effector to measure the force between the palm handle and the distal wrist link. Several auxiliary parallel links and zero free-length springs, made up of tension springs, cables and pulleys, are utilized to keep the exoskeleton in gravity balanced state based on the hybrid method carried out by Agrawal and Fattah [16]. The principle of gravity balance has been analyzed in our previous research [17]. Lengths of the upper arm and forearm links are designed to be adjustable for the users with a height between 1.6m~2.0m. The exoskeleton is connected to the user by using a soft cuff attached to the places near the elbow and upper arm. For safety consideration, mechanical end stops are located on each joint disk to guarantee that the robot cannot exceed the maximum workspace. In addition, two dead-man buttons are held by the patient and therapist such that a single push can stop the system immediately in an emergency.

B. Configuration space kinematics

The structure of the rehabilitation device is required to match the range of motion (ROM) of human arm in ADL. The kinematics parameters described in Denavit-Hartenburg (D-H) convention [18] are shown in Table. I and Fig. 3. For the purpose of reducing the kinematics complexity, the base frame of the proposed upper-limb exoskeleton is moved from the experimental platform to the first shoulder joint, as the ROM of the passive mobile platform is quite limited during therapy treatment. According to the D-H parameters, the position and orientation of the end-effector can be determined. The transformation from the base frame to the end-effector can be written as:

$$ {}^{b}T_{e} = {}^{b}T_{1}(\theta_1)\,{}^{1}T_{2}(\theta_2)\,{}^{2}T_{3}(\theta_3)\,{}^{3}T_{4}(\theta_4)\,{}^{4}T_{e}(\theta_5) \tag{1} $$

where ${}^{i}T_{j}$ denotes the 4×4 transformation matrix derived from D-H convention. θ_j represents the joint rotation variable. The forward kinematics is a function of joint variables and limb lengths L_1 and L_2.

For the purpose of establishing the relations between, on one side, the human-robot interaction forces at the end-effector and, on the other side, the driving torque of each active joint, the Jacobian matrix of the upper-limb exoskeleton is deduced based on the vector product method [19] as follows:

$$ J = \begin{bmatrix} \mathbf{z}_1 \times {}^{1}\mathbf{p}_5^0 & \mathbf{z}_2 \times {}^{2}\mathbf{p}_5^0 & \cdots & \mathbf{z}_5 \times {}^{5}\mathbf{p}_5^0 \\ \mathbf{z}_1 & \mathbf{z}_2 & \cdots & \mathbf{z}_5 \end{bmatrix} \tag{2} $$

where $\mathbf{z}_i$ denotes unit vector corresponding to each joint axis. ${}^{i}\mathbf{p}_5^0$ represents the vector from the origin of {i} coordinate to the origin of {5} coordinate.

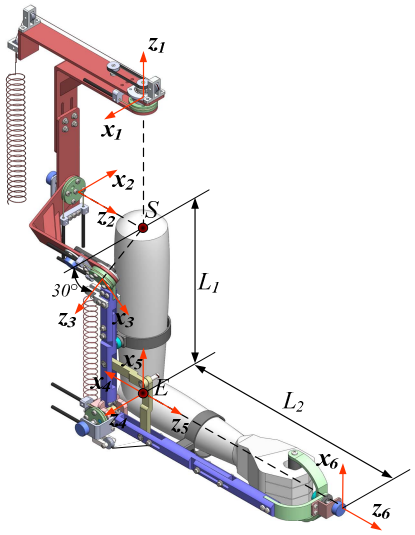

Fig. 3. D-H link frame assignment for the upper-limb exoskeleton.

TABLE I. D-H PARAMETERS FOR THE UPPER-LIMB EXOSKELETON

link i	θ_i (deg)	ROM (robot)	ROM (ADL)	α_i (deg)	d_i (mm)	a_i (mm)
1	θ_1	150~240	130~245	90	0	0
2	θ_2	-180~-45	-195~-35	90	0	0
3	θ_3	-120~30	-135~45	30	$L_1/2$	0
4	θ_4	-30~-180	-45~-180	90	0	0
5	θ_5	-85~60	-90~75	0	L_2	0

C. Singularity Placement

Shoulder joint will reach a singular configuration when the three rotational axes become coplanar. The singularities should be moved to the boundaries of the desired workplace. In order to analyze and optimize the overall mechanical design, it is necessary to develop a simple method to calculate the singularity level W at each configuration in the accessible workspace [20]. W can be computed as:

$$W = 1 - \left|\mathbf{z_1} \cdot (\mathbf{z_2} \times \mathbf{z_3})\right| \tag{3}$$

Here $\mathbf{z_i}$ represents the unit vector corresponding to each joint axe. When the singularity level is equal to 0, the joint axes are orthogonal and the manipulability of the mechanism is the best; conversely, a degree of freedom is lost or compromised when the singularity level is equal to 1.

The three shoulder axes are mutually perpendicular to each other in our previous design. However, as a result, the singular configurations can be achieved through abduction by 90 degrees, and that is smaller than the ROM in ADL. Thus, a modified design is promoted to eliminate these singularities from the desired workplace, where the flexion/extension joint configuration of the shoulder is located at an angle of 30 degrees with respect to the horizontal plane, as shown in Fig. 3. Fig. 4 shows the available workspace and singularity level distribution of the elbow in the modified design. Point S denotes the spherical joint of the shoulder. It can be seen that the location points with high singularity level are distributed on the top of the workplace.

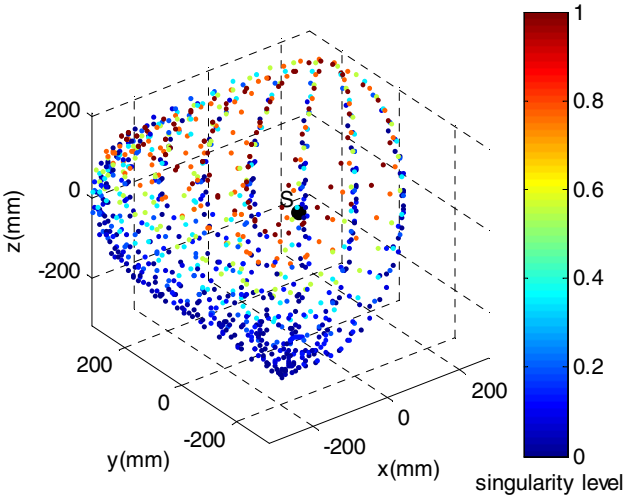

Fig. 4. Accessible workspace and singularity level distribution of the elbow in the modified design

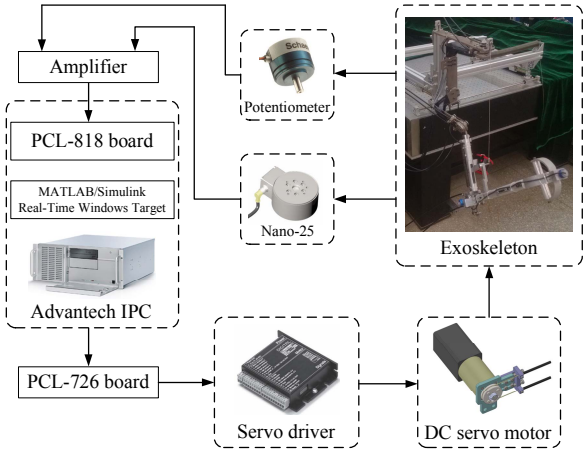

Fig. 5. Experimental setup and control system

III. CONTROL SYSTEM

A Matlab/RTW-based real-time control system is established in xPC target environment and used for the control of the upper-limb rehabilitation exoskeleton. The hardware architecture of the control system is shown in Fig. 5. The real-time control system mainly consists of two industrial personal computers (IPC-610H, Advantech Inc.) working as the host computer and the xPC target, a three axes strain gauge-type force/torque sensor installed at the end-effector to measure the human-robot interaction forces, potentiometers mounted at the robot joints to measure the angular positions and velocities, and several servo drivers used in actuation of the DC motors. An xPC target compatible A/D acquisition card (PCL-818, Advantech Inc.) is made used to acquire and process the feedback signals measured from the force/torque sensor and potentiometers and amplified by a transistor made power amplifier. Bessel low-pass analog filters with a cut-off frequency of 200 rad/s are implemented in the controller to filtrate the interaction force and joint position signals. The time critical control algorithms for rehabilitation training are firstly

developed in host computer in the Simulink environment and then transmitted to the xPC target through serial port. The xPC target is capable of analyzing all the feedback information and sending the appropriate commands to each motor driver with a sampling time of 1ms. The servo motors are run in torque control mode to provide expected driving torques. The generated commands are transformed into analog output signals by using a D/A card (PCL-726, Advantech Inc.). The developed real-time control system provides a convenient software environment for the developers and therapists to evaluate the effectiveness of rehabilitation training with different control strategies.

IV. Control Experiments and Results

A. Impedance control

An impedance controller is applied to the rehabilitation training system to assist the stroke patients in regaining their motor abilities. The controller is comprised of an inner force feedback loop and an outer position feedback loop, the diagram is shown in Fig. 6. The exact trajectory of the moving task is defined by the therapist according to the individual impairment of patient. The robotic assistance can be modified according to the muscular residual abilities and recovery progress of the patient by analyzing the human-robot interaction forces at the end-effector. For the serve stroke patients, it is quite difficult to actively move their own upper limb and perform the therapy tasks. In this case, the impedance of the control scheme is set to a high value in order to increase the robotic assistance and help the patient to move his/her own limb in accordance with the preset trajectories. For the mild stroke patients, the recovery is more effective if rehabilitation process actively involve the intention of the subject into therapy training. Therefore, the impedance of the control scheme is set to a low value in this case, for the purpose of decreasing the robotic assistance and allowing the patient to deviate from the preset trajectories [21].

The impedance control strategy is capable of developing a mass-damper-spring relationship between the position of the end-effector and the force applied on the user. The desired force at the end-effector can be computed as:

$$\mathbf{F_d} = (M_d s^2 + B_d s + K_d)\mathbf{e} \tag{4}$$

$$\mathbf{e} = \mathbf{X_d} - \mathbf{X} \tag{5}$$

where $\mathbf{F_d}$ is the desired force applied on the hand of user; M_d, B_d, and K_d denote the control inertia, damping, and stiffness of the system; $\mathbf{X_d}$ and $\mathbf{X}$ represent the planning and actual position of the end-effector; $\mathbf{e}$ denotes the position error.

The control torque of each driving motor is given by the transpose Jacobian of the exoskeleton:

$$\boldsymbol{\tau}_c = J^T(\mathbf{F_d} - \mathbf{F}) + \boldsymbol{\tau}_f \tag{6}$$

where $\boldsymbol{\tau}_c$ is control torque; $\mathbf{F}$ represents the actual interaction force at the end-effector; J^T is the transpose Jacobian of the exoskeleton; $\boldsymbol{\tau}_f$ denotes the friction torque coming from the robot joint and Bowden-cable transmission system. Since the exoskeleton system keeps in gravity balanced state during operation, the gravity of the system is eliminated in the developed control algorithm.

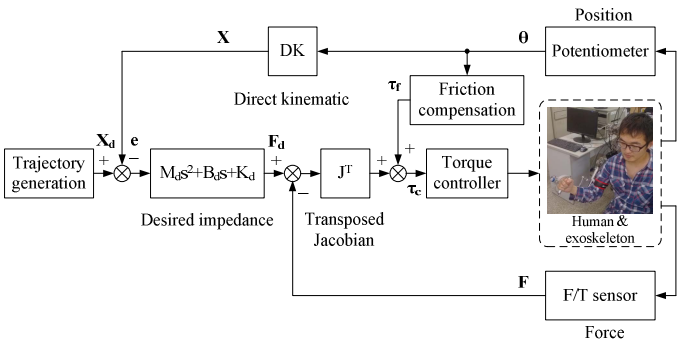

Fig. 6. The impedance control scheme of the upper-limb exoskeleton in the reaching task

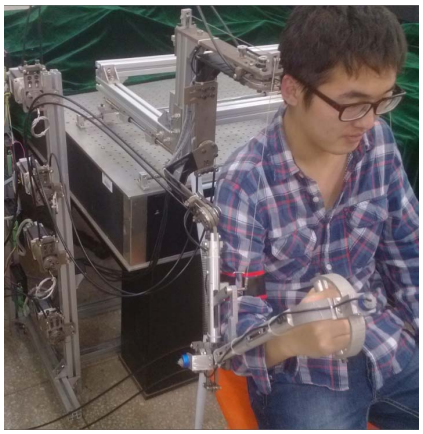

Fig. 7. Rehabilitation training with the upper-limb exoskeleton

B. Experiments and results

A first prototype of the proposed upper limb rehabilitation exoskeleton has been installed at the Southeast University in China, as shown in Fig. 7. Several preliminary experiments have been implemented on a healthy subject in order to identify the basic functional features for the rehabilitation training and, in addition, ensure that human-robot interaction is natural and comfortable in practical application. In the experiments, the user was required to perform the shoulder internal/external rotation movement in two different training modes. The first- and second-order derivative elements of the impedance model are sensitive to the variation of position errors and, as a result, reduce the robustness of the system. Therefore, for control simplicity, the effects of damping and inertia were neglected during experiment. The desired impedance of the control system was then converted to a zero-order function of the joint angle (i.e. M_d=0, B_d=0, F_d=$K_d \cdot \mathbf{e}$), which was known as stiffness control [22].

In the first training mode, trajectory tracking experiments with different stiffness parameters were carried out to test the impedance controller. The experimental results are presented comparatively in Fig. 8. The shoulder internal/external rotation joint of the exoskeleton was commanded to follow a sinusoid wave trajectory with a frequency of 0.25 Hz and amplitude of 30 degrees. Firstly, the exoskeleton conducted the training task without the subject. The joint desired position θ_d was input as the reference trajectory and the parameter θ_{out} represented the actual output position of robot joint. The stiffness parameter

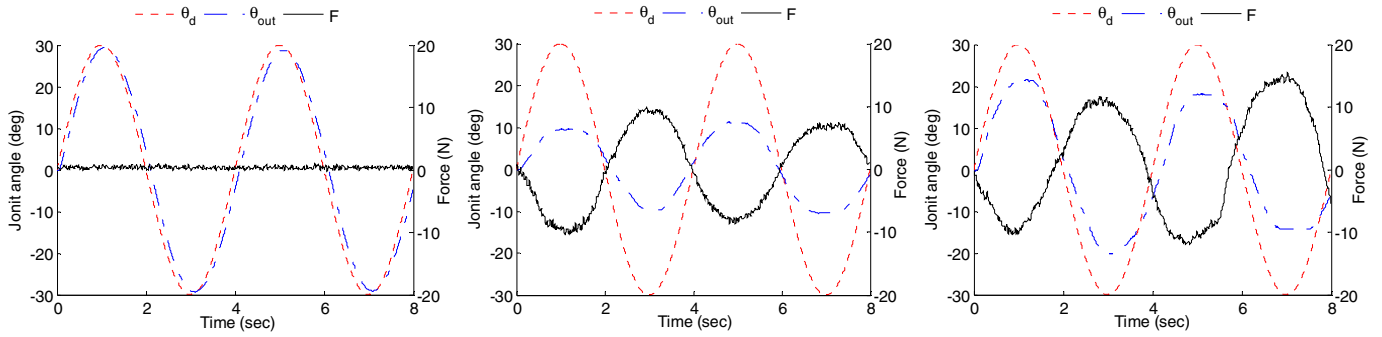

(a) no external force, K_d=800 N/m (b) K_d=800 N/m (c) K_d=2000 N/m

Fig. 8. Trajectory tracking experiments with different impedance parameters.

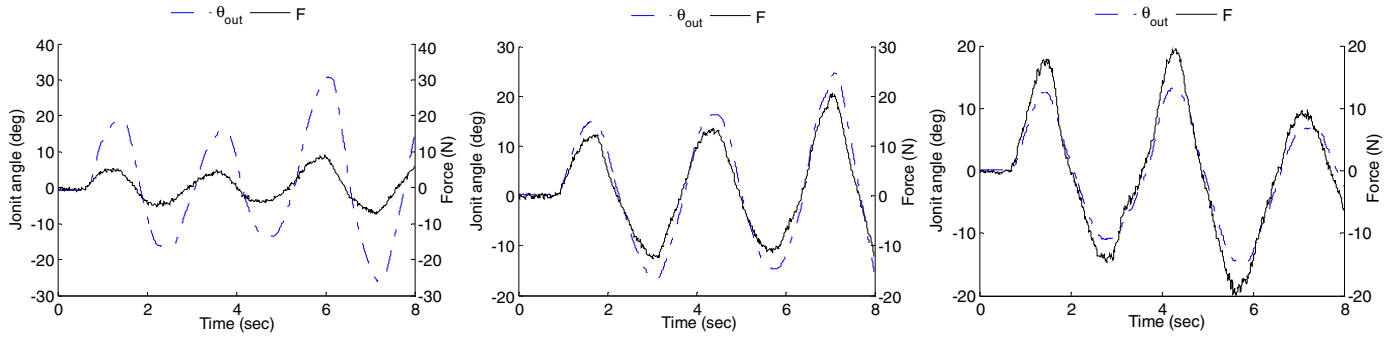

(a) K_d=400 N/m (b) K_d=800 N/m (c) K_d=2000 N/m

Fig. 9. Active moving experiments with different impedance

K_d was set to 800 N/m. From Fig. 8(a), it is clear to see that the output position can accurately follow the input reference without external force applying on the end-effector. Secondly, the subject was equipped with the rehabilitation device with his right-hand palm grasping the handle at the end-effector, allowing the robot to drag his/her hand and accomplish the moving task passively. The stiffness parameter K_d was set to 800 N/m and 2000 N/m, respectively. The output positions and interaction forces in the movement direction are shown in Fig. 8(b) and Fig. 8 (c). Note that the interaction force introduced tracking deviation in the human-robot interactive procedure and, as a result, protect the patient from excessive traction force. The deviation is concerned with the stiffness value of the impedance model: a small stiffness value may cause a large tracking error during operation.

In the second training mode, the device was desired to stay at the original location (i.e. θ_d=0). The subject grasped the handle and performed the moving experiment actively. If the deviation from the original position increases, an adjustable force will be applied on the hand of subject to force it return to the original location. Fig. 9 describes the results of the active moving experiments, where the stiffness parameter was set to 400 N/m, 800 N/m, and 2000 N/m, respectively. As can be observed, the changing tendency of robot joint position is basically consistent with that of the interaction force and, besides, the increase of stiffness value will reduce deviation under the same external force. In other words, the robot joint acts like a single torsion spring during experiment. By changing the stiffness value of the impedance model, the system compliance of the rehabilitation device can be adjusted and applied to the patients with different weakness levels.

V. Conclusion and Future Works

A gravity balanced upper limb exoskeleton with Bowden-cable actuators was developed in this paper, which can be used for the stroke patients to regain their motor functions. The application of Bowden-cable actuators helps to simplify the mechanical structure design and achieve a lightweight and low consumption system. The major mechanical structure and the kinematics of the exoskeleton were described and optimized to achieve full-workspace in ADL. For the control of the robotic system, a real-time control system was established in xPC target environment based on Matlab/RTW. An impedance control strategy has been developed to execute the therapy training tasks. Several preliminary experiments were carried out to verify the effectiveness of the proposed device and control algorithm. Future work is to improve the impedance control strategy and demonstrate that the therapeutic result of upper limb rehabilitation with the proposed device is better than that delivered by physical therapist.

Acknowledgment

This research has been supported by the Fundamental Research Funds for the Central Universities (CXZZ13_0085) and the China Nation Nature Science Foundation under grant 51175078 and 50875044.

References

[1] E. S. Lawrence, C. Coshall, R. Dundas, J. Stewart, A. G. Rudd, R. Howard, and C. D. Wolfe, “Estimates of the prevalence of acute stroke impairments and disability in a multiethnic population,”Stroke, vol. 32, no. 6, pp. 1279–1284, Jun. 2001

[2] G. Kwakkel, B. J. Kollen, and H. I. Krebs, "Effects of robot-assisted therapy on upper limb recovery after stroke: A systematic review," Neurorehabil. Neural Repair, vol. 22, no. 2, pp. 111–121, 2008.

[3] N. Hogan, H. I. Krebs, J. Charnnarong, et al, "MIT-MANUS: a workstation for manual therapy and training II," Applications in Optical Science and Engineering. International Society for Optics and Photonics, pp. 28-34, 1993.

[4] P. S. Lum, C. G. Burgar, M. Van der Loos, et al, "MIME robotic device for upper-limb neurorehabilitation in subacute stroke subjects: A follow-up study," Journal of rehabilitation research & development, vol. 43(5), pp. 631-642, 2006.

[5] T. Nef, M. Mihelj, G. Colombo, and R. Riener, "ARMin-Robot for Rehabilitation of the Upper Extremities," IEEE International Conference on Robotics and Automation. pp. 3152-3157, May. 2006.

[6] C. Carignan, J. Tang, and S. Roderick, "Development of an exoskeleton haptic interface for virtual task training," Intelligent IEEE/ International Conference on Robots and Systems. pp. 3697-3702. Oct. 2009.

[7] Michnik, Andrzej, et al, "Control System for a Limb Rehabilitation Robot," Information Technologies in Biomedicine," Springer Berlin Heidelberg, pp. 423-430. 2010.

[8] S. Coote, E. Stokes, B. Murphy, and W. Harwin, "The effect of GENTLE/s robot-mediated therapy on upper extremity dysfunctionpost stroke," Proceedings of the 8th International Conference on Rehabilitation Robotics, pp.59–61. April, 2003.

[9] A. Frisoli, F. Salsedo, M. Bergamasco, et al, "A force-feedback exoskeleton for upper-limb rehabilitation in virtual reality," Applied Bionics and Biomechanics, vol. 6(2), pp. 115-126, 2009.

[10] L. Q. Zhang, H. S. Park, and Y. Ren, "Developing an intelligent robotic arm for stroke rehabilitation," IEEE 10th International Conference on Rehabilitation Robotics, pp. 984-993, 2007

[11] T. Rahman, W. Sample, R. Seliktar, M. Alexander, and M. Scavina, "A Body-Powered Functional Upper Limb Orthosis," Journal of Rehabilitation Research and Development, vol. 37(6), pp. 675–680, 2000.

[12] J. L. Herder, "Development of a Statically Balanced Arm Support: ARMON," International Conference on Rehabilitation Robotics, pp. 281-286, 2005.

[13] A. H. Stienen, E. E. Hekman, G. B. Prange, M. J. Jannink, A. M. Aalsma, F. C. van der Helm, and H. van der Kooij, "Dampace: Design of an exoskeleton for force-coordination training in upper-extremity rehabilitation," Journal of medical devices, vol. 3(3), pp. 1-10, 2009.

[14] Schiele, and F. C. T. Van Der Helm, "Kinematic Design to Improve Ergonomics in Human Machine Interaction," IEEE Transactions on Neural Systems and Rehabilitation Engineering, vol. 14(4), pp. 456-469, 2006.

[15] T. Nef, and R. Riener, "Shoulder actuation mechanisms for arm rehabilitation exoskeletons," Biomedical Robotics and Biomechatronics, 2nd IEEE RAS & EMBS International Conference, pp. 862-868, 2008.

[16] S. K. Agrawal, and A. Fattah, "Gravity-balancing of spatial robotic manipulator," Mechanism Machine. Theory, vol. 39(12), pp. 1331–1344, 2004.

[17] Q. C. Wu, and X. S. Wang, "Design of a gravity balanced upper limb exoskeleton with bowden cable actuators," 2013 IFAC Symposium on Mechatronic Systems, pp. 679–683, 2013.

[18] B. Siciliano, "Kinematic control of redundant robot manipulators: A tutorial," J. Intell. Robot. Syst., vol. 3, no. 3, pp. 201–212, 1990.

[19] X. Wenming, W. hongtao, L. Xiang, and Z. Jianying, "Study of new analytic solution of robotic relative Jacobian matrix," Journal of Southeast University (Natural Science Edition), Vol.32 no.4, pp. 1-6, 2002.

[20] S. J. Ball, I. E. Brown, and S. H. Scott, "MEDARM: a rehabilitation robot with 5DOF at the shoulder complex," 2007 IEEE/ASME international conference on Advanced intelligent mechatronics, pp. 1-6, 2007.

[21] S. Hussain, S. Q. Xie, and P. K. Jamwal, "Adaptive impedance control of a robotic orthosis for gait rehabilitation", IEEE Transactions on Cybernetics, vol. 43(3), pp. 1025-1034, 2013.

[22] Y. Yang, L. Wang, J. Tong, et al, "Arm rehabilitation robot impedance control and experimentation," IEEE International Conference on Robotics and Biomimetics , pp. 914-918, 2006.

[23] M. S. Ju, C. C. K. Lin, D. H. Lin, et al, "A rehabilitation robot with force-position hybrid fuzzy controller: hybrid fuzzy control of rehabilitation robot," IEEE Transactions on Neural Systems and Rehabilitation Engineering, vol. 13(3), pp. 349-358, 2005.

[24] L. Chen, and X. S. Wang, "Inverse transmission model and compensation control of a single–tendon–sheath actuator," IEEE Transactions on Industrial Electronics, vol. 61(3), pp. 1424-1433, 2014.